New Phytologist

Arabidopsis IRT3 is a zinc-regulated and plasma membrane localized zinc/iron transporter

Ya-Fen Lin[1], Hong-Ming Liang[1], Shu-Yi Yang[1], Annegret Boch[2], Stephan Clemens[2,3], Chyi-Chuann Chen[1], Jing-Fen Wu[4], Jing-Ling Huang[1] and Kuo-Chen Yeh[1]

[1]Agricultural Biotechnology Research Center, Academia Sinica, Taipei, Taiwan, Republic of China; [2]Leibniz-Institut für Pflanzenbiochemie, Halle, Germany; [3]Department of Plant Physiology, University of Bayreuth, Bayreuth, Germany; [4]Institute of Plant and Microbial Biology, Academia Sinica, Taiwan, Republic of China

Author for correspondence:
Kuo-Chen Yeh
Tel: 886 2 2789 8630
Email: kcyeh@gate.sinica.edu.tw

Received: *18 October 2008*
Accepted: *16 December 2008*

New Phytologist (2009) **182**: 392–404
doi: 10.1111/j.1469-8137.2009.02766.x

Key words: *Arabidopsis halleri*, hyperaccumulator, IRT3, zinc (Zn) homeostasis, ZIP transporter.

Summary

• ZIP transporters (ZRT, IRT-like proteins) are involved in the transport of iron (Fe), zinc (Zn) and other divalent metal cations. The expression of IRT3, a ZIP transporter, is higher in the Zn/cadmium (Cd) hyperaccumulator *Arabidopsis halleri* than is that of its ortholog in *Arabidopsis thaliana*, which implies a positive association of its expression with Zn accumulation in *A. halleri*.

• *IRT3* genes from both *A. halleri* and *A. thaliana* functionally complemented the Zn uptake mutant *Spzrt1* in *Schizosaccharomyces pombe*; and Zn uptake double mutant *zrt1zrt2*, Fe-uptake mutant *fet3fet4* and conferred Zn and Fe uptake activity in *Saccharomyces cerevisiae*. By contrast, the manganese (Mn) uptake mutant *smf1* phenotypes were not rescued. Insufficient Cd uptake for toxicity was found.

• Expression of IRT3-green fluorescent protein (GFP) fusion proteins in Arabidopsis root protoplasts indicated localization of both IRT3 proteins in the plasma membrane.

• Overexpressing *AtIRT3* in *A. thaliana* led to increased accumulation of Zn in the shoot and Fe in the root of transgenic lines. Therefore, IRT3 functions as a Zn and Fe-uptake transporter in Arabidopsis.

Introduction

Plants require transition metals for normal growth and development. These transition metals, such as iron (Fe), copper (Cu), manganese (Mn) and zinc (Zn), are essential for many redox reactions and play a structural role in many proteins. For example, Zn is a catalytic or structural cofactor for many enzymes and proteins, including the ubiquitous Zn-finger DNA binding proteins (Vallee & Auld, 1990; Rhodes & Klug, 1993). Because Zn is essential for many biochemical processes, cells need to maintain intracellular Zn concentrations at a physiologically adequate level, even when the extracellular Zn supply is very low. To accomplish this, cells need an efficient system of Zn uptake transporters on the plasma membrane. However, to avoid the toxicity from excess Zn, cells also must develop mechanisms to control the intracellular concentration of Zn, including efflux of additional Zn out of the cell or sequestration into subcellular compartments. Previous studies have shown that the successful maintenance of Zn homeostasis in whole plants greatly relies on the coordinated regulation of the uptake transporters, members of the ZRT, IRT-like proteins (ZIP), natural resistance-associated macrophage protein (Nramp) families, the efflux transporters, and members of the P_{1B}-ATPase and cation diffusion facilitator (CDF) families (Colangelo & Guerinot, 2006).

The ZIP transporters are involved in the transport of Zn, Fe, Mn and cadmium (Cd). Individual transporters differ in substrate range and specificity (Guerinot, 2000; Maser *et al.*, 2001). *AtIRT1*, the first member of the ZIP family identified, was cloned from *Arabidopsis* by functional complementation of an iron uptake-deficient yeast mutant, *fet3 fet4* (Eide *et al.*, 1996). IRT1 is considered to be the main transporter for high-affinity iron (Fe^{2+}) uptake in roots (Vert *et al.*, 2002). Plants overexpressing *AtIRT1* also accumulate higher levels of Cd and Zn than wild-type plants do under Fe starvation, which indicates that AtIRT1 can also transport these metals (Connolly *et al.*, 2002). This finding is also supported by transport studies in yeast (Eide *et al.*, 1996; Korshunova *et al.*, 1999). Like the expression of *AtIRT1*, that of *AtIRT2* is

induced under Fe-deficient conditions. However, AtIRT2 can transport only Zn and Fe in yeast but not Mn and Cd (Vert *et al.*, 2001). *AtZIP1* and *AtZIP3* from *Arabidopsis* can complement Zn uptake in the yeast Zn uptake mutant *zrt1zrt2*, are upregulated in the root in response to Zn deficiency and are proposed to play a role in Zn transport from soil to the plant (Grotz *et al.*, 1998). Although the expression of *AtZIP4* was shown to be regulated by Zn, it shows Cu transport and regulation characteristics (Wintz *et al.*, 2003).

Homologues of *ZIP* have also been found in other species, including both dicotyledonous and monocotyledonous plants. *TcZNT1*, from the Zn/Cd hyperaccumulator *Thlaspi caerulescens*, mediated high-affinity Zn uptake and low-affinity Cd uptake when expressed in yeast (Pence *et al.*, 2000). A study of *ZNT1* expression and high-affinity Zn uptake in roots of *T. caerulescens* and in a related nonaccumulator, *Thlaspi arvense*, showed that alteration in the regulation of *ZNT1* gene expression by plant Zn status results in increased Zn influx in roots. *TcZNT1* and *TcZNT2* were predominantly expressed in roots, although their expression was barely responsive to Zn. By contrast, these genes were expressed only under conditions of Zn deficiency in the nonaccumulator *T. arvense* (Assuncao *et al.*, 2001). *GmZIP1* from soybean was found to be highly selective for Zn, whereas Cd inhibited Zn uptake in yeast cells expressing *GmZIP1* (Moreau *et al.*, 2002). In the model legume *Medicago truncatula*, *MtZIP1*, *MtZIP5*, and *MtZIP6* complemented a Zn uptake yeast mutant, *MtZIP4* and *MtZIP7* complemented an Mn uptake yeast mutant and *MtZIP3*, *MtZIP5* and *MtZIP6* complemented an Fe uptake yeast mutant (Lopez-Millan *et al.*, 2004). These data imply that these proteins function in *M. truncatula* as metal transporters with different metal specificity. Recently, *OsIRT1* was defined as a homolog of *AtIRT1* and functions as an Fe transporter upregulated by Fe deficiency (Bughio *et al.*, 2002; Ishimaru *et al.*, 2006). OsZIP1, OsZIP3 and OsZIP4 were found to be functional Zn transporters in rice (Ramesh *et al.*, 2003; Ishimaru *et al.*, 2005). However, the expression of *OsZIP4* responds to Zn deficiency, whereas *OsZIP1* responds to Cu deficiency (Ishimaru *et al.*, 2005). Thus, the roles and functions of the *ZIP* family members are multiple and diverse for heavy metal homeostasis.

Arabidopsis halleri ssp. *halleri* has been known as a Zn hyperaccumulator (Ernst, 1974). Even on noncontaminated soil, *A. halleri* was found to contain substantially higher amounts of Zn in shoots than in roots (Bert *et al.*, 2002). *Arabidopsis halleri* has also been shown to be a Cd hyperaccumulator. Field samples of *A. halleri* were found to contain >100 μg g^{-1} DW Cd and have a shoot-to-root Cd ratio > 1 (Baker & Brooks, 1989; Dahmani-Muller *et al.*, 2001). Similar properties were found in another subspecies, *A. halleri* ssp. *gemmifera,* from Japan (Kubota & Takenaka, 2003; Chiang *et al.*, 2006). In previous genomic studies, the predominant expression of the ZIP transporters *AhIRT3*, *AhZIP3*, *AhZIP6* and *AhZIP12* in shoots and roots and *AhZIP9* in roots of *A. halleri* was suggested to be responsible for the Zn/Cd uptake ability in this hyperaccumulator (Becher *et al.*, 2004; Weber *et al.*, 2004; Chiang *et al.*, 2006).

However, the functional analysis of these ZIPs in *A. halleri* is limited. *AtIRT3* in *A. thaliana* was found and named previously because of its sequence similarity to *AtIRT1* (Eide *et al.*, 1996). According to a later report, the *AtIRT3* sequence is more similar to that of *AtZIP4* (Grotz *et al.*, 1998). The expression of *AtIRT3* can respond to Zn but not to Cd, Cu or Na (Talke *et al.*, 2006), which implies a possible role for IRT3 in Zn transport and homeostasis. Here, we report on the functional study of the *IRT3* genes *AhIRT3* and *AtIRT3* from *A. halleri* ssp. *gemmifera* and *A. thaliana*, respectively. The possible contributions of IRT3 to Zn hypertolerance and hyperaccumulation in *A. halleri* are discussed.

Materials and Methods

Gene cloning and sequencing

To clone *AhIRT3*, total RNA was extracted from *A. halleri* ssp. *gemmifera* with use of TRIzol reagent (Invitrogen, Carlsbad, CA, USA). First-strand cDNA was synthesized with the oligo-dT (5′-(T)24VN-3′) primer from l μg of total RNA with use of Superscript II reverse transcriptase (Invitrogen). Primers designed according to the sequence of *AtIRT3* were used for polymerase chain reaction (PCR) amplification of full-length *AhIRT3*. A SMART RACE (rapid amplification of cDNA ends) cDNA amplification kit (BD Biosciences Clontech, Palo Alto, CA, USA) was used for cloning the 5′ and 3′ extended sequence. The RACE-Ready cDNA samples were diluted 10 times with tricine-ethylenediaminetetraacetic acid (EDTA) buffer for the subsequent RACE-PCR reaction. Two gene-specific primers, 5′-TCCAGAGGCAATGGCTG-CTACTTCA-3′ and 5′-GCAACCAAGGGAACAACA-ATACCCG-3′, were designed according to the *AhIRT3* sequence for use in 5′ and 3′ RACE, respectively.

To express *IRT3* genes in *Schizosaccharomyces pombe*, *AtIRT3* (containing 1.2-kb of full-length coding sequence) was PCR amplified from cDNA by use of a 5′ primer (5′-GAGTCGACAATGTTCTTCGTCGATGTTCTTT-3′) with a *Sal*I restriction site, and a 3′ primer (5′-AGGAGCG-GTTAAGCCCAAATGGCAAGAGAA-3′) with a *Bsr*BI restriction site. The PCR fragment was restricted with *Sal*I and *Bsr*BI and cloned into the pSLF173 (Forsburg & Sherman, 1997) vector for expression in *S. pombe*. The same strategy was used to clone *AhIRT3* into pSLF173 with a 5′ primer (5′-GACTCGAGAATGGCTGCTACTTCATCTAAT-3′) containing an *Xho*I site and a 3′ primer (5′-AGGAGCGGT-TAAGCCCAAATGGCAAGAGAA-3′) containing a *Bsr*BI site.

To express *IRT3* genes in *Saccharomyces cerevisiae*, a *Not*I PCR fragment of the *AtIRT3* 1.2-kb of full-length coding sequence was amplified, restricted and cloned into the pFL61

vector with a 5′ primer (5′-GAGCGGCCGCATGTTCTTCGTCGATGTTCTTT-3′) and a 3′ primer (5′-AGGCGGCCGCTTAAGCCCAAATGGCAAGAGAA-3′) containing a designed *Not*I site for expression in *S. cerevisiae*. The same strategy was employed to clone *AhIRT3* into pFL61 with a 5′ primer (5′-GAGCGGCCGCATGGCTGCTACTTCATCTAAT-3′) and a 3′ primer (5′-AGGCGGCCGCTTAAGCCCAAATGGCAAGAGAA-3′), and *AtIRT1* with a 5′ primer (5′-GAGCGGCCGCATGAAAACAATCTTCCTCGTAC-3′) and a 3′ primer (5′-AGGCGGCCGCTTAAGCCCATTTGGCGATAATCGACAT-3′).

To construct *C*-terminal green fluorescent protein (GFP) fusion with AtIRT3, the full-length *AtIRT3* coding region was PCR amplified with a 5′ primer (5′-AGTCTAGAATGTTCTTCGTCGATGTTCTTT-3′) and a 3′ primer (5′-ATGGATCCAAGCCCAAATGGCAAGA-3′), restricted and cloned into *Xba*I and *Bam*HI sites of p326GFP to create the in-frame fusion of *AtIRT3* and *GFP*, designated AtIRT3/326GFP. A 5′ primer (5′-AGTCTAGAATGGCTGCTACTTCATCTAATGTT-3′) and a 3′ primer (5′-ATGGATCCAAGCCCAAATGGCAAGG-3′) were used for AhIRT3/326GFP cloning.

We used the CaMV35S promoter to drive overexpression of *AtIRT3* in *A. thaliana*. A PCR fragment of full-length *AtIRT3* coding sequence was PCR amplified with a 5′ primer (5′-GAACATGTTCTTCGTCGATGTTCTTTGG-3′) and a 3′ primer (5′-AGCACGTGTTAAGCCCAAATGGCAAGAGAAGA-3′), restricted with *Pci*I and *Pml*I, and cloned into the *Nco*I and *Pml*I sites of pCAMBIA1305.1. To examine the promoter activity of AtIRT3, of 597 bp, the 528 bp upstream sequence of AtIRT3 5′-UTR containing the promoter and partial 5′-UTR regions according to the annotation in The Arabidopsis Information Resource was PCR amplified with a 5′ primer (5′-GAAAGCTTGTATGATGTATTATTGCAAATTTGC-3′) containing a *Hin*dIII site and a 3′ primer (5′-GACCATGGAAATATGAGAATCAGACAGATC-3′) containing a *Nco*I site, then restricted and cloned into pCAMBIA305.1 to create P_{AtIRT3}:GUS (ß-glucuronidase)/pCAMBIA1305.1 for the promoter activity assay.

Prediction of transmembrane topology

Sequence alignment and phylogenic tree were analyzed with Biology WorkBench at San Diego Supercomputer Center, CA, USA (http://workbench.sdsc.edu/). The Phobius web server (http://phobius.cbr.su.se/) was used to predict transmembrane domains (Kall *et al.*, 2007).

Yeast growth and transformation

The *S. cerevisiae* strains ZHY3, DDY4, *smf1* and BY4741, were grown and transformed as previously described (Rogers *et al.*, 2000) under the selection of *URA* on the plasmids pFL61 and derivatives with *AtIRT1*, *AtIRT3* and *AhIRT3*. The transformed yeast strains were grown on synthetic defined media (SD) supplemented with 20 g l^{-1} D-glucose and necessary auxotrophic supplements for complementation test. YPD media were used for growth control of stains examined. In growth-test experiments, 5-μl drops of yeast culture at an optical density of 1, 0.1, 0.01 and 0.001 were spotted onto medium. Yeast strains of *zrt1zrt2* ZHY3 (*MATα ade6 can1 his3 leu2 trp1 ura3 zrt1::LEU2 zrt2::HIS3)* were grown on SD/–ura medium (pH 5.8) supplemented with 1 mM EDTA and 0, 0.5 or 0.75 mM $ZnCl_2$. Yeast strains of *fet3fet4* DDY4 (*MATa can1 his3 leu2 trp1 ura3 fet3::HIS3 fet4::LEU2*) were grown on SD/–ura medium (pH 5.5, 5.7 or 6, containing 50 mM 2-(*N*-morpholino) ethanesulfonic acid (MES)) supplemented with 0, 50, 100 or 200 μM $FeCl_3$. Yeast strains of *smf1* (BY4741; *MATa his3 leu2 met15 ura3 YOL122c::kanMX4*) were grown on SD/–ura medium (pH 5.8) containing 0 or 5 mM ethylene glycol-*bis*(beta-aminoethyl ether)-*N*,*N*,*N*′,*N*′-tetraacetic acid (EGTA). The yeast wild-type strains BY4741 (*MATa his3 leu2 met15 ura3*) were grown on SD/–ura medium (pH 6) containing 0, 5, or 10 μM $CdCl_2$.

The *S. pombe* strains, wild-type and *Spzrt1* mutant harboring with the empty vector pSLF173 and *IRT3* genes, were grown in Edinburgh minimal medium (EMM) plus 1 μM thiamine as described previously (Boch *et al.*, 2008). Expression of IRT3 genes was under the control of the *nmt1* promoter, which is suppressed by thiamine. A concentration of 1 μM in the medium results in low expression levels. For growth assays, cells were first cultivated in EMM + thiamine + 20 μM Zn^{2+}, then harvested, washed with H_2O and diluted to an optical density (OD) of 0.05 into Zn^{2+}-free EMM + thiamine, supplemented with different Zn^{2+} concentrations. Growth was determined after 22 h.

$^{65}Zn^{2+}$-uptake assays

Zinc uptake assays were performed with *S. cerevisiae zrt1zrt2* expressing *AtIRT1*, *AtIRT3* or *AhIRT3* in pFL61 as described by Zhao & Eide (1996). Stationary-phase cultures were diluted to $OD_{600} = 0.3$ in SD/–ura medium containing 1 mM EDTA and grown to an exponential growth phase. Cells were washed once in uptake buffer (10 mM MES, 2% (w : v) glucose, pH 6.1), and cell density was adjusted to 1×10^6 cells per 0.5 ml ($OD_{600} = 0.4$). The uptake assay was started by adding Zn^{2+} containing $^{65}Zn^{2+}$ (final concentration 10 μM). Cells were incubated at 30°C in a shaking water bath, and 0.5 ml samples were filtered through nitrocellulose membranes (0.45 μM) at the indicated times. Filters were washed with 10 ml of ice-cold SSW (1 mM Na-EDTA, 5 mM $MgCl_2$, 1 mM $CaCl_2$, 1 mM KH_2PO_4, 20 mM Na_3-citrate, pH 4.2). Cell-associated $^{65}Zn^{2+}$ was measured by use of a liquid scintillation counter (LS6500; Beckman, Munich, Germany).

Competition studies were done in parallel by adding 10 μM $^{65}Zn^{2+}$ (control) or 10 μM $^{65}Zn^{2+}$ plus 20 μM of $FeCl_2$. An amount of 1 mM Na-ascorbate was added to the $FeCl_2$ culture and its control to keep Fe in a reduced state. After 5 min, 0.5 ml samples were filtered and washed as above.

Plant materials, growth conditions and transformation

Asexual propagation of *A. halleri* ssp. *gemmifera* seedlings from Fumuro, Japan, were as described previously (Chiang *et al.*, 2006). *A. halleri* cuttings at the six-leaf stage were transferred to new phytagel media for 2 wk to generate roots. Both *A. halleri* and *A. thaliana* (ecotype *Columbia*-0) were cultured in the growth chamber with light intensity at 70 μmol m^{-2} s^{-1} under a 16-h light : 8-h dark cycle at 22°C. To detect *IRT3* expression, rooted *A. halleri* or *A. thaliana* seedlings were grown for 4 wk or 2 wk, respectively, in half-strength Murashige and Skoog (MS) phytagel media, then transferred to normal (half-strength MS), iron-deficient (lack of iron with additional 100 μM FerroZine), Zn-deficient (lack of $ZnSO_4$) and excess Zn (additional 100 μM $ZnSO_4$ for *A. thaliana* and 1 mM $ZnSO_4$ for *A. halleri*) media for 5 d. *Agrobacterium tumefaciens* strain GV3101 harboring the plasmid 35S:AtIRT3/pCAMBIA1305.1 was used to transform *A. thaliana*, Col-0, by *in planta* transformation. Fourteen-day-old Arabidopsis root tissues were used for protoplast isolation modified from the methods for mesophyll protoplasts (Sheen, 2001); http://genetics.mgh.harvard.edu/sheenweb/protocols_reg/protocols_reg_.php). Instead of cutting leaf tissue, we cut roots to small pieces before cell wall digestion.

For localization experiments, p326GFP, AtIRT3/326GFP and AhIRT3/326GFP were introduced separately into root protoplasts with solution consisting of 40% polyethylene glycol (PEG) 4000, 0.2 M mannitol and 0.1 M $CaCl_2$. After transfection, the protoplasts were incubated in a Zn-deficient condition (W5 solution with 10 μM *N*,*N*,*N*′,*N*′-Tetrakis-(2-pyridylmethyl)-ethylenediamine (TPEN); Sigma, St Louis, MO, USA) in the dark at room temperature overnight before observation by confocal microscopy.

Metal analysis

Roots and shoots were harvested separately and washed with 10 mM $CaCl_2$ for 20 min and H_2O for 10 min. Samples were dried at 70°C for 3 d. Shoot samples (*c.* 60 mg) and root samples (*c.* 20 mg) from 25 plants were transferred into a Teflon vessel and digested with 2 ml 65% HNO_3 and 0.5 ml H_2O_2 (both Suprapur; Merck, Darmstadt, Germany) in a MarsXpress microwave digestion system (CEM, Matthews, NC, USA). Tomato leaves (SRM-1573a) from the National Institute of Standards and Technology (Gaithersburg, MD, USA) were used as a reference. The volume of the solution after digestion was adjusted to 8 ml with H_2O and filtered by use of a 0.45-μm membrane filter. The concentrations of Mn, Cu, Zn, Fe, Mo, Mg and Ca in digested samples were analysed by use of inductively coupled plasma-optical emission spectrometry (ICP-OES) (OPTIMA 5300; Perkin-Elmer, Wellesley, MA, USA). The concentration of each element in the sample was determined in triplicate.

Confocal microscopy and GUS staining

The GFP fluorescence of root protoplasts transfected with AtIRT3/326GFP and AhIRT3/326GFP was observed on confocal laser scanning microscopy (LSM 510 META; Carl Zeiss, Jena, Germany). The samples were visualized with excitation set at 488 nm and emission signal recovered between 500 and 530 nm for GFP, and excitation at 543 nm and emission signal recovered above 560 nm for autofluorescence signal. For GUS staining, plant tissues were incubated in GUS solution containing 100 mM sodium phosphate (pH 7.0), 1 mg ml^{-1} 5-bromo-4-chloro-3-indoyl-β-D-glucuronide (X-Gluc), 0.5 mM potassium ferricyanide, 0.5 mM potassium ferrocyanide, 10 mM EDTA, and 0.1% Triton X-100 at 37°C for 5 h or 16 h. The stained tissues were sequentially bleached with 50%, 75% and 95% ethyl alcohol to remove chlorophyll. For histological observations, stained roots and leaves of 18-d-old P_{AtIRT3}:GUS transgenic plants (1 × 1 mm) were dehydrated in a graded ethanol series and embedded in LR white resin (London Resin Company, London, UK). Then the block was trimmed and cut in thin cross-sections (3 μm) by use of a Leica UltraCut E microtome (Leica, Solms, Germany). Cross-sections were observed with a AXIO Imager Z1 (Carl Zeiss) and photographed with a digital camera AxioCam HRc (Carl Zeiss).

RNA isolation, reverse transcriptase (RT)-PCR and quantitative real-time PCR (Q-PCR)

Total RNA from *A. halleri*- or *A. thaliana*-treated tissue was isolated by use of the pine tree method as described (Chang *et al.*, 1993). One-microgram samples of total RNA were used for synthesizing cDNA. For RT-PCR, transcript-specific primers for 5′ (5′-TCTCAGCAACAGAGTCCATTT-3′) and 3′ (5′-GGTTGTGAGGGCGAAAAAA-3′) were designed for the amplification of a 962-bp fragment for each gene. Polymerase chain reaction (PCR) was performed in cycles of 30 s at 94°C, 30 s at 55°C and 60 s at 72°C. The Q-PCR procedure was described previously (Chiang *et al.*, 2006). Primers 5′-GCCCTCACAACCCCGATAG-3′ and 5′-GCTCCGACACTGTGAGAATTGA-3′ were used for the detection of *AtIRT3* expression; and 5′-GCCCTCACAA-GCCCGATA-3′ and 5′-TGCTCCGACGCTGTGAGA-3′ for *AhIRT3*. Actin8 was chosen as an internal control because of its stable expression and high homology in both species. To ensure similar PCR efficiency for both species, we used the same pair of primers for this actin8 control, 5′-TTACCCGA-CGGACAAGTGATC-3′ and 5′-ATGATGGCTGGA-

AAAGGACTTC-3′, to detect high-homology short targets. In several Zn treatments, actin8 was expressed similarly and was within one-cycle difference in both species. The Q-PCR involved at least two biological replicates. The efficiency tests for the use of primers and data calculation followed the manufacturer's instructions (ABI PRISM 7000; Applied Biosystems, Foster City, CA, USA).

Statistical analysis

Data were expressed as mean ± SD. An unpaired two-tailed *t*-test was used to analyse significant differences between controls and treatments.

Results

Cloning and phylogenetic analysis of IRT3 gene in *A. halleri* and *A. thaliana*

To characterize the *IRT3* in *A. halleri*, cDNA corresponding to *IRT3* was cloned by RT-PCR from leaf tissues of *A. halleri* ssp. *gemmifera*. Primers were designed according to the sequence of the *AtIRT3* coding region for the amplification of *AhIRT3* cDNA. The 5′ and 3′ sequences were obtained by use of RACE, as described in the Materials and Methods section. The deduced amino acid sequence of AhIRT3 was 381 amino acids. AhIRT3 contains eight predicted transmembrane domains, similar to AtIRT1, AtIRT2 and AtIRT3, and a histidine-rich putative metal-binding domain with high similarity to AtIRT3 (91% identity) and AhZIP4 (78% identity) (Vert *et al.*, 2001). The amino acid residue E103 in AtIRT1 suggested to be responsible for Zn transport (Rogers *et al.*, 2000) is conserved in AhIRT3, but the Fe- and Mn-responsible residue D100 of AtIRT1 is not conserved in AhIRT3. Sequence alignment of AtIRT1, AtIRT2, AtIRT3, AtZIP4 and AhIRT3 indicated that AhIRT3 protein has the highest sequence homology to AtIRT3 protein apart from a deletion in the *N*-terminus (Fig. 1). The phylogenetic tree of available *ZIP* and *IRT* gene sequences revealed all known *IRT* or *ZIP* genes from both *A. halleri* and *A. thaliana* clustered together as pairs (see the Supporting Information, Fig. S1). It also showed that the *IRT3*s and the Fe-regulated transporters *IRT1*s/*IRT2*s belong to distinct phylogenetic clades. By contrast, *IRT3* clustered closely with *ZIP4*s and several *ZNT* transporter genes from *Thlaspi* species, which implies that *IRT3*s may be functionally more related to Zn transporters.

IRT3 behaves as a Zn and Fe uptake transporter in yeast

As a first step for the functional characterization of IRT3 proteins, we tested whether *IRT3* genes can complement *S. pombe* and *S. cerevisiae* mutants. Both *AtIRT3* and *AhIRT3* complemented the Zn uptake deficiency of a *S. pombe* mutant strain disrupted in *SpZrt1* (Boch *et al.*, 2008). Unlike mutant cells carrying the empty vector, cells expressing AtIRT3 or AhIRT3 were able to grow at low external Zn concentrations supplied in regular media (Fig. 2).

To further examine the uptake activity of other metals, we also tested whether *IRT3* genes can complement other *S. cerevisiae* mutants. As shown in Fig. 3, both *AtIRT3* and *AhIRT3* complement the Zn uptake-deficient double mutant *zrt1zrt2* as efficiently as does *AtIRT1*. Interestingly, both *IRT3* genes can complement *fet3fet4* at low pH but not at high pH conditions (Fig. S2). Neither *AtIRT3* nor *AhIRT3* confers the ability to take up Mn thus unable to complement the *smf1* mutant. When expressed in a wild-type strain BY4741, in contrast to the expression of *AtIRT1*, no toxicity phenotype was seen in yeast cells expressing *AtIRT3* and *AhIRT3* in the presence of Cd (Fig. 3c,d). Thus, *IRT3* genes from both Arabidopsis species function similarly in yeast and are potential Zn and Fe transporters. However, the Fe transport activity of AtIRT3 and AhIRT3 is much less than or different from that of AtIRT1.

Following yeast complementation studies, we tested AtIRT3 and AhIRT3 expressed in *S. cerevisiae zrt1zrt2* for their ^{65}Zn uptake activity. We performed the uptake experiments in the presence of 10 μM Zn as a substrate. *AtIRT3*- and *AhIRT3*-dependent Zn uptake was low at the pH condition used but still significantly different from that of the empty vector control (Fig. 4a). AtIRT1 was used as a positive control. The Zn uptake activity of AtIRT3 and AhIRT3 was comparable to that mediated by AtIRT1 for 20 min after the addition of Zn.

On the basis of complementation results, to investigate Fe uptake ability of the two heterologously expressed IRT3 proteins, we tested competition by Fe in comparison with that in AtIRT1. Figure 4b shows that ^{65}Zn uptake was strongly inhibited with Fe by *c.* 50% for all three proteins tested.

The ^{65}Zn uptake ability of AtIRT3 and AhIRT3 and Fe inhibition of the uptake further support the proteins' abilities in the uptake of Zn and Fe in yeast (Fig. 3). More detailed kinetic analyses are needed to reveal the full biochemical properties of these two transporters, but these are currently beyond the scope of the present study.

IRT3 is localized in the plasma membrane

To characterize the subcellular localization of IRT3 proteins in plant cells, CaMV35S promoter-driven chimeric genes encoding a *C*-terminal GFP fusion of AtIRT3 and AhIRT3 proteins were constructed. The recombinant DNA was purified and transfected into *A. thaliana* root protoplasts for transient expression. The GFP signals for both constructs of AtIRT3–GFP and AhIRT3–GFP were enriched on the plasma membrane, whereas cytosolic GFP remained only in the cytoplasm (Fig. 5). Together with yeast complementation data, this finding suggests that both IRT3 proteins function as Zn and Fe-uptake transporters in the plasma membrane.

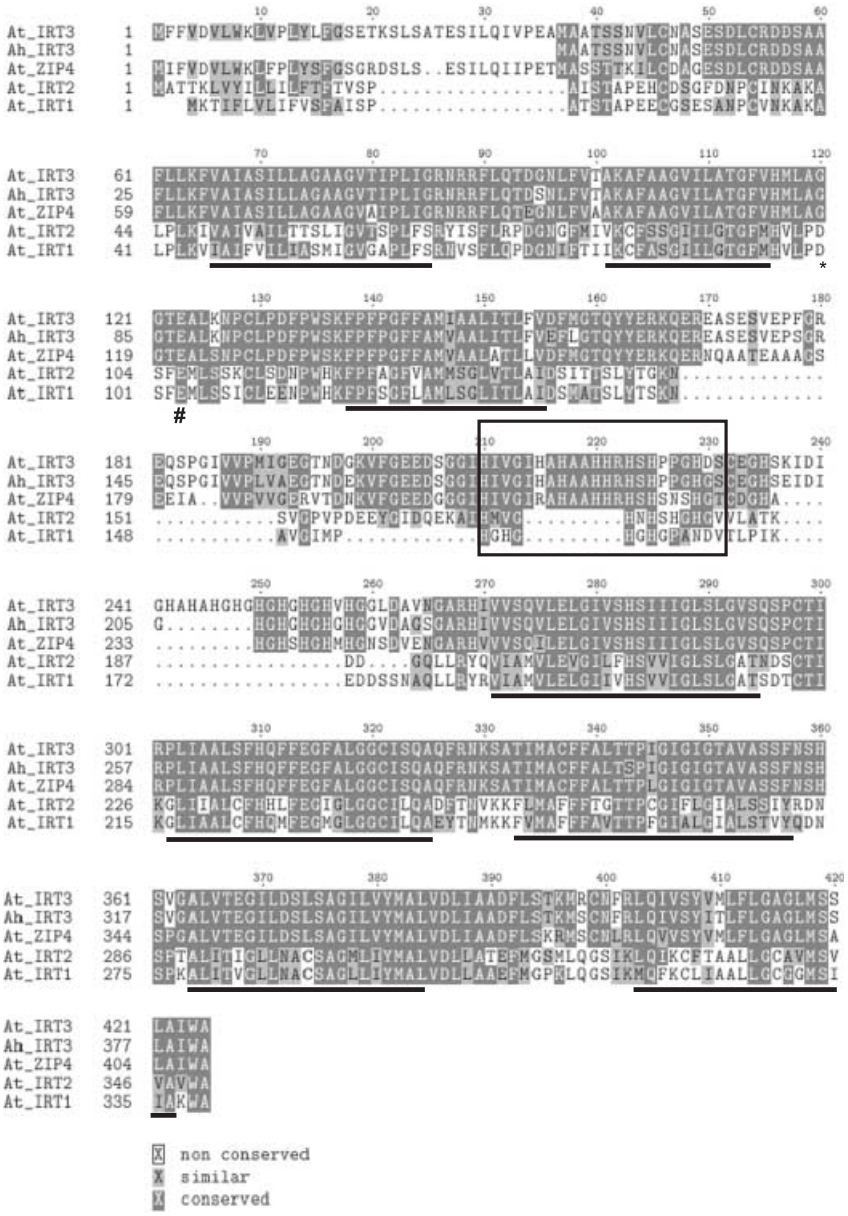

Fig. 1 Sequence alignment of AtIRT3 and AhIRT3 with plant ZIP proteins. Amino acid sequences of *Arabidopsis thaliana* At_IRT1 (At4g19690.2), At_IRT2 (At4g19680.1), At_IRT3 (At1g60960.1), At_ZIP4 (At1g10970.1) and *Arabidopsis halleri* Ah_IRT3 (AY960758) are listed. Regions of the putative transmembrane domains according to the annotation of AtIRT1 are underlined (Rogers *et al*., 2000). The putative metal-binding domain is boxed and the residues D100 and E103 of AtIRT1 are marked * and #, respectively.

Expression pattern of *IRT3* in *A. thaliana* and *A. halleri*

Using Q-PCR, we investigated the expression of *IRT3* genes in both *A. thaliana* and *A. halleri* under different Zn and Fe conditions. In general, the expression of *IRT3* was higher in *A. halleri* than in *A. thaliana.* Under normal conditions, *AhIRT3* was expressed approx. threefold higher than *AtIRT3* in both root and shoot tissues. Both *AtIRT3* and *AhIRT3* could be induced under Zn-deficient conditions and repressed by excess Zn (Fig. S3). Moreover, under Zn-deficient conditions, *AtIRT3* in *A. thaliana* was induced to a substantially higher level in shoots than roots, reaching an expression level similar to or higher than that of *AhIRT3* in *A. halleri*. This Zn regulation of *IRT3* expression is consistent between *A. halleri* ssp. *gemmifera* (this study) and *A. halleri* ssp. *halleri* (Talke *et al*., 2006).

To examine the expression pattern of *AtIRT3*, a 597 bp fragment upstream of *AtIRT3*, containing the putative promoter region (528 bp) of intergenic sequences (633 bp) and partial 5′UTR, was fused with a GUS reporter gene for transforming *A. thaliana*. Among 12 transgenic lines checked, nine lines showed GUS activity. One of the nine lines showed weak GUS activity. The GUS staining indicated that the *AtIRT3* promoter was constitutively expressed in all tissues and at all stages (Fig. 6a,c,e,g,i,k,m). Histochemical studies revealed that GUS activity was downregulated under excess Zn and upregulated under Zn deficiency in seven P_{AtIRT3}*:GUS* transgenic plants but not in $P_{CaMV35S}$*:GUS* transgenic plants

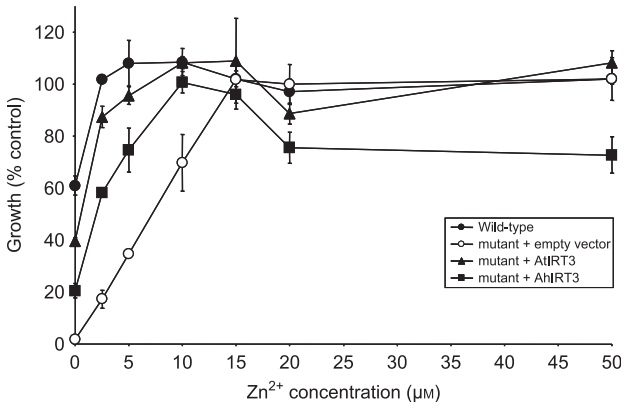

Fig. 2 Growth of *Schizosaccharomyces pombe* cells disrupted in the *SpZrt1* gene and carrying the empty pSLF173 (open circles), pSLF173-AtIRT3 (triangles) or pSLF173-AhIRT3 (squares) construct monitored in Edinburgh's minimal medium (EMM) supplemented with zinc (Zn^{2+}) concentrations as indicated. As a control, an isogenic wild-type strain (closed circles) was also examined.

and one of eight lines with strong GUS activity (Fig. S4). Although GUS activities of plants grown under different Zn conditions do not differ greatly, the data suggest that transcriptional regulation may be involved in the differential *IRT3* transcript accumulation in response to environmental Zn availability.

Detailed cytohistology confirmed the ubiquitous activity of the *AtIRT3* promoter in all living cell types in leaf, including guard cells (Fig. 6o) and trichomes (data not shown). A similar phenomenon was also observed in the root (Fig. 6p) and root hairs (data not shown). The *AtIRT3* promoter was especially active in root stele, and GUS activity was clear in passage cells (Fig. 6p).

Metal concentrations of *A. thaliana* overexpressing *AtIRT3*

From the results described, we conclude that AtIRT3 and AhIRT3 share qualitatively comparable biochemical properties in metal transport. To investigate whether the high expression of *IRT3* contributes to high accumulation of Zn, we constructed *A. thaliana* transgenic lines heterologously overexpressing *AtIRT3* driven by a CaMV35S promoter. The expression of *AtIRT3* in the root and shoot of four transgenic lines was confirmed by RT-PCR (Fig. 7a). The transgenic lines showed no obvious phenotype. The dry weight of these transgenic lines did not significantly change under Zn treatments (Fig. S5). Metal content analysis indicated that roots in all four lines accumulated Zn levels similar to that of the wild-type when grown in the normal condition (Fig. 7b). Two lines, OE2-6 and OE6-7, with relatively high expression of *AtIRT3* (Fig. 7a), accumulated substantially higher levels of Zn (up to 25% more) in shoots than did the wild type (Fig. 7b). Intriguingly, the level of Fe was markedly higher (by more than twofold in OE2-6) in the roots of all transgenic lines than in wild-type roots (Fig. 7b). The concentrations of additional divalent essential metals, Mn, Cu, Mo, Mg and Ca, were also comparable in the root and shoot of wild-type and transgenic lines (Fig. S6).

Taken together, these data indicate that the increased expression of *AtIRT3* specifically resulted in high levels of Zn accumulation in the shoot and Fe accumulation in the root without affecting the accumulation of Mn, Cu, Mo, Mg or Ca.

Discussion

IRT3 is a member of the *ZIP* gene family comprising 15 transporters in *A. thaliana* (Guerinot, 2000). In this study, we demonstrated that both *AtIRT3* and *AhIRT3* function as Zn uptake systems when expressed in both *S. pombe* and *S. cerevisiae*. The transporters complemented Zn and Fe uptake-deficient *S. cerevisiae* mutants but not Mn and Cd uptake (toxicity) phenotypes. More importantly, *AtIRT3*- and *AhIRT3*-expressing yeast cells showed higher ^{65}Zn uptake activity (Fig. 4). This activity was inhibited by the addition of Fe, which suggests the proteins' ability to transport Zn and Fe. In addition, *A. thaliana* transgenic lines overexpressing *AtIRT3* accumulated more Zn in the shoot and Fe in the root than did the wild-type (Fig. 7). These data suggest that IRT3 is more likely a Zn and Fe transporter in Arabidopsis. The evidence that both AtIRT3 and AhIRT3 are targeted to the plasma membrane supports a role in Zn and Fe uptake.

Members of the ZIP family have eight predicted transmembrane (TM) domains (Guerinot, 2000). AtIRT1 can transport multiple substrates, including Fe^{2+}, Mn^{2+}, Zn^{2+}, Cd^{2+} and Co^{2+} (Rogers *et al.*, 2000; Vert *et al.*, 2002). By exchanging amino acid residues in some inter-TM domains, the metal ion selectivity can be altered in AtIRT1 (Rogers *et al.*, 2000). For example, the D100A mutant of AtIRT1 lacks the ability to transport Fe and Mn. The region containing the D100 residue is not conserved between IRT1 and the two IRT3 proteins from *A. thaliana* and *A. halleri* (Fig. 1), which may explain in part why IRT3 does not transport Mn and has low Fe transport activity in the yeast system. Overexpression of *AtIRT3* indeed increases Fe accumulation in the root tissues. Elevated Fe accumulation was observed in Arabidopsis by overexpressing an AtIRT1 mutant defective in Fe-induced turnover. Transport of Fe might also be a rate-limiting step in Strategy-I plants (Kerkeb *et al.*, 2008). Therefore, the simplest explanation is that when expressed at high levels, AtIRT3 can transport Fe in plants, although secondary effects exerting an indirect influence on Fe homeostasis cannot be ruled out.

The E103 residue of IRT1, suggested as an important residue for selectivity to Zn, is indeed conserved in *IRT3* genes (Fig. 1). These observations support the notion that transporter selectivity in the ZIP family has evolved from changes in

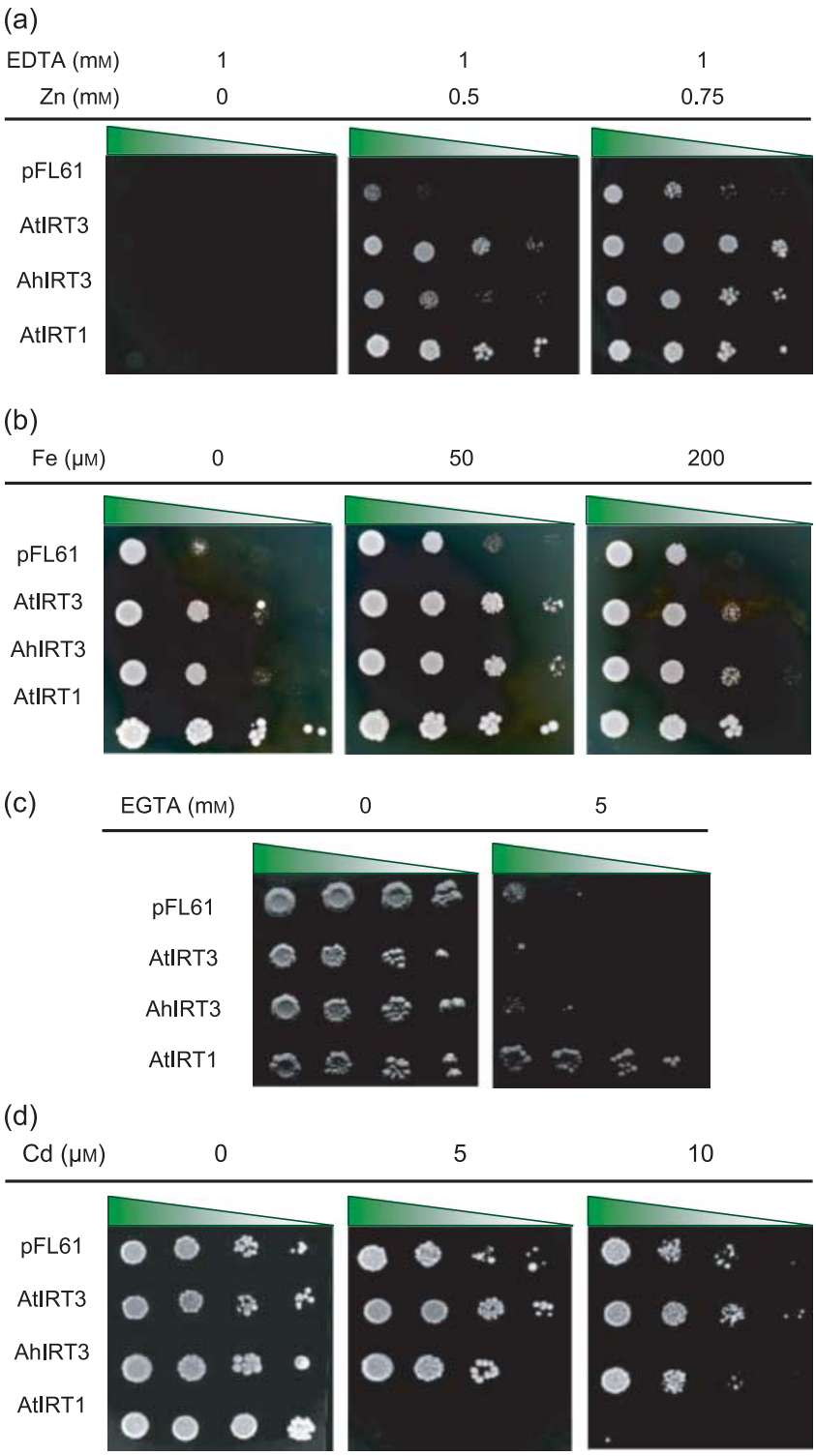

Fig. 3 Complementation of *Saccharomyces cerevisiae* mutants (a) *zrt1zrt2*, (b) *fet3fet4*, (c) *smf* and (d) wild-type strain BY4741. Cells carrying *AtIRT1*, *AtIRT3* and *AhIRT3* in the vector pFL61 were grown under different heavy-metal conditions as indicated. The gradient marks above each panel indicate cell dilutions from concentrated (left) to diluted (right).

the region between TM2 and TM3 (Rogers *et al.*, 2000). The histidine-rich region between TM3 and TM4 has been suggested to be a metal-binding domain. However, IRT3 and IRT1/IRT2 proteins show much variation in the region between TM3 and TM4 (Fig. 1). Whether this domain is involved in cation selectivity remains to be studied. The Zn-regulated Zn transporters (ZNT), found in the *Thlaspi* species, are closely clustered together with IRT3 (Fig. S1), which suggests that these genes may have evolved from the same ancestral molecule or by functional selection.

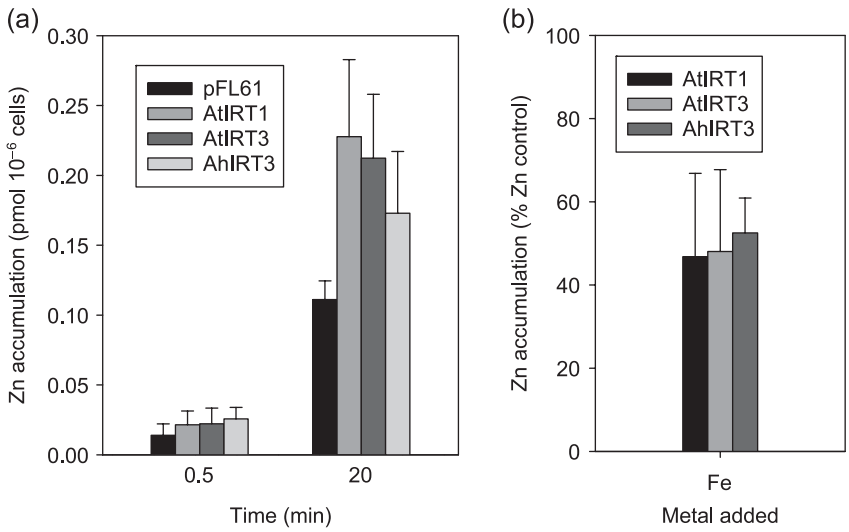

Fig. 4 (a) Both AtIRT3 and AhIRT3 mediate zinc (Zn^{2+}) uptake activity in *Saccharomyces cerevisiae*. Zinc accumulation by *S. cerevisiae zrt1zrt2* cells expressing either *AtIRT3* or *AhIRT3* in comparison with *AtIRT1* as a positive control and the empty vector control (pFL61). Uptake was assayed using $^{65}Zn^{2+}$. Final Zn^{2+} concentration was 10 μM. Error bars represent the standard error of means from four independent experiments. The *t*-test analyses reveal a significant difference in Zn accumulation in 20 min between the vector control and AtIRT1, AtIRT3 and AhIRT3, with $P = 0.02$, 0.02 and 0.06, respectively. (b) Effect of Fe on *IRT3*-dependent Zn^{2+} uptake. Zinc uptake of cells expressing *AtIRT1*, *AtIRT3*, *AhIRT3* or the empty vector pFL61 was assayed in the presence of a twofold excess of iron (Fe^{2+}). Zinc uptake, determined using $^{65}Zn^{2+}$, is shown as the percentage of the control culture assayed in the absence of excess Fe^{2+}. The mean control values were 0.215, 0.111 and 0.071 pmol 10^{-6} cells per 5 min for *AtIRT1*, *AtIRT3* and AhIRT3, respectively. Error bars represent the standard deviation for means from three independent experiments.

The expression of *IRT3* in *A. thaliana* is ubiquitous and responsive to Zn status (Fig. 6), which suggests that IRT3 is involved in the Zn homeostasis in most cell types. However, the expression of *AtIRT3* in passage cells (Fig. 6p) implies the possible contribution of AtIRT3 to loading Zn for long-distance transport (Peterson & Enstone, 1996).

The Zn regulation of *AhIRT3* expression suggests that *A. halleri* ssp. *gemmifera* responds to Zn concentrations in the environment to control uptake. Similar Zn regulation was also observed in *A. halleri* ssp. *halleri* (Talke *et al.*, 2006). In our promoter–GUS fusion study, promoter activity was slightly regulated by the Zn condition (Fig. S4), which suggests that promoter-based transcriptional regulation is involved in the *IRT3* expression. We also conducted the promoter assays with both 528 bp and 1 kb promoter fragments in an luciferase-based transient assay system. Consistent with our observation, excess Zn represses and deficient Zn induces the expression of reporter genes driven by the 528 bp or 1 kb *AtIRT3* promoters. However, the regulation of both constructs was subtle but significant, as seen in a GUS assay of the 528 bp *AtIRT3* promoter (data not shown). Although additional regulatory elements may exist within the structure gene or flanking sequence not included in our promoter fusion, detailed promoter analysis will be required to conclude the activity of the promoter.

In addition, a post-transcriptional regulation in addition to the transcriptional regulation might exist for the control of *IRT3* expression. Post-transcriptional and translational regulations have been observed in the regulation of the Fe uptake-related genes *IRT1* and *FRO2* (Connolly *et al.*, 2002, 2003). Two lysine residues of putative ubiquitination on AtIRT1 were found recently. These residues play a crucial role in Fe induced turnover of IRT1 (Kerkeb *et al.*, 2008). Indeed, one of the residues, lysine146, is conserved in both AhIRT3 and AtIRT3. Although IRT3 is a member of the ZIP family, as is IRT1, whether a complicated regulation system including transcriptional and post-transcriptional mechanisms is involved in the uptake and homeostasis of Zn is still unclear. Suitable antibodies will be required to investigate the detailed regulation of *IRT3* expression.

A metallophyte such as *A. halleri* often grows in soil that contains certain metals in vast excess over others (e.g. Zn concentrations > 1 mg g^{-1}). However, the acquisition and distribution of other essential metals such as Fe must be maintained. Thus, one might expect to find selection for altered metal specificity in transporters of such species. However, the growth phenotypes of various yeast mutants expressing the two proteins showed no notable difference in metal ion selectivity (Fig. 3). Consistent with previous findings (Talke *et al.*, 2006), our data also indicate a higher expression of *IRT3* in *A. halleri* than in *A. thaliana* under normal conditions (Fig. S3). A possible mechanism for the high expression of *IRT3* in *A. halleri* is expression of sequestration or efflux transporters such as MTPs or HMAs creating

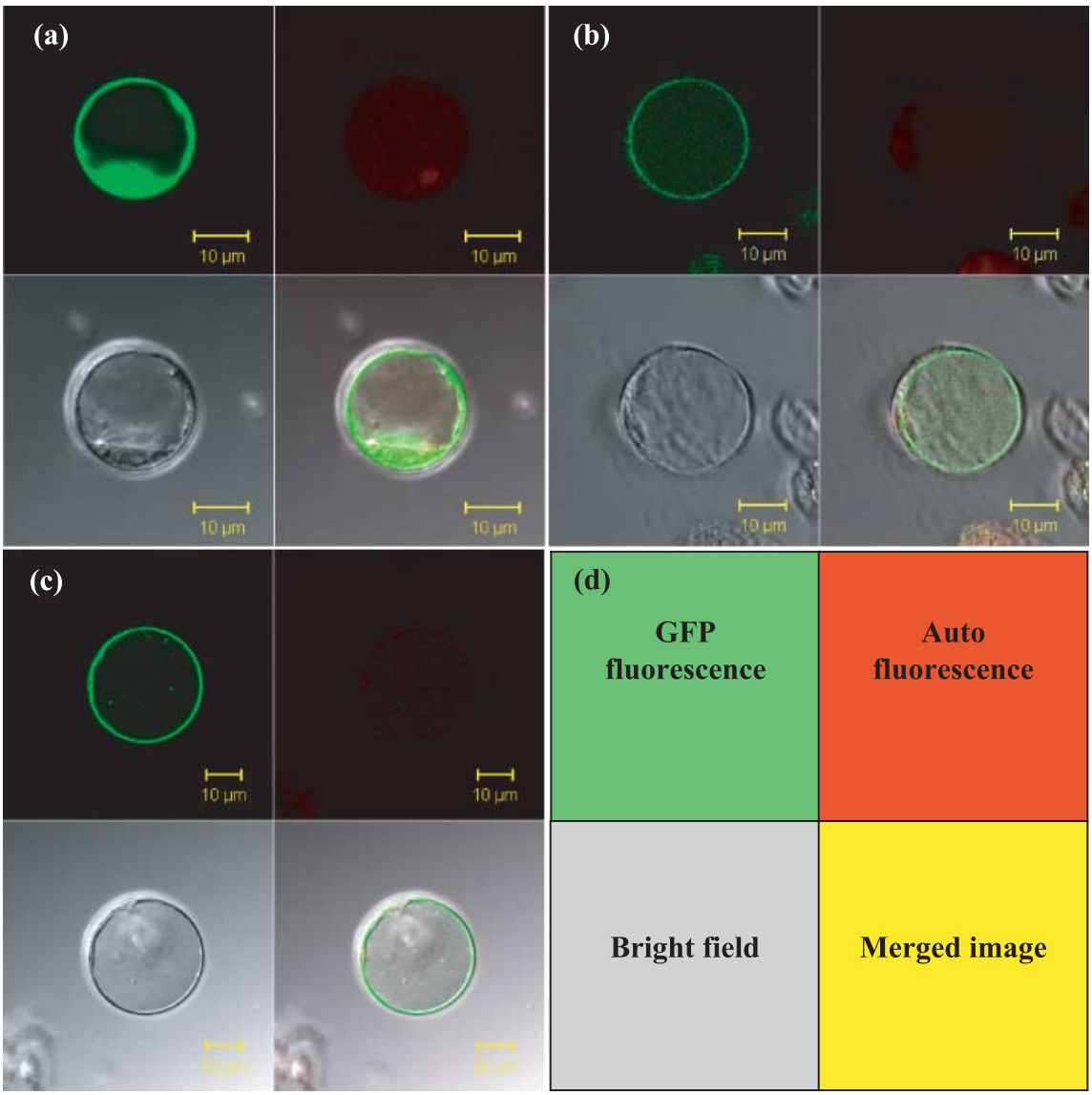

Fig. 5 Plasma membrane localization of IRT3 proteins. The fluorescence of heterologously expressed cytosolic green fluorescent protein (GFP) (a), or IRT3–GFP fusion proteins, AtIRT3-GFP (b) and AhIRT3-GFP (c) in root protoplasts was detected by confocal microscopy. The image quadruplets (d) represent GFP-specific signal (excitation, 488 nm, emission, 500–530 nm), autofluorescence (excitation, 543 nm, emission, > 560 nm), bright field and a merged image of the three previous images. Bars, 10 μm.

Zn-deficient intracellular conditions, which in turn upregulates the expression of the uptake transporters, including IRT3. Indeed, Hanikenne *et al.* recently found that knocking down *HMA4* abolished the high expression of *IRT3* and *ZIP4* in *A. halleri* (Hanikenne *et al.*, 2008). These data suggest that *HMA4* is needed to achieve the high expression of members of the *ZIP* family in the root of *A. halleri* (Hanikenne *et al.*, 2008). A similar *HMA4*-dependent upregulation of *IRT3* was observed in the root of *A. thaliana* (Hanikenne *et al.*, 2008). Increased Zn accumulation was reported in *HMA4*-overexpression lines, possibly because of the enhanced expression of *IRT3*. Our results further support this notion by the significantly greater Zn accumulation of transgenic *A. thaliana* overexpressing *IRT3* (Fig. 7b). Interestingly, overexpression of *IRT3* also enhanced the accumulation of Fe in the root of the transgenic plants (Fig. 7b). The high expression of *IRT3* in *A. halleri* may also be involved in proper Fe acquisition under conditions of Zn excess.

An in-depth mechanistic study of Zn hyperaccumulation is crucial for effective use of plant Zn hyperaccumulation in phytoremediation. In the current study, we present the identification and molecular characterization of a Zn-regulated *ZIP* member, *IRT3*. By overexpressing this gene in a

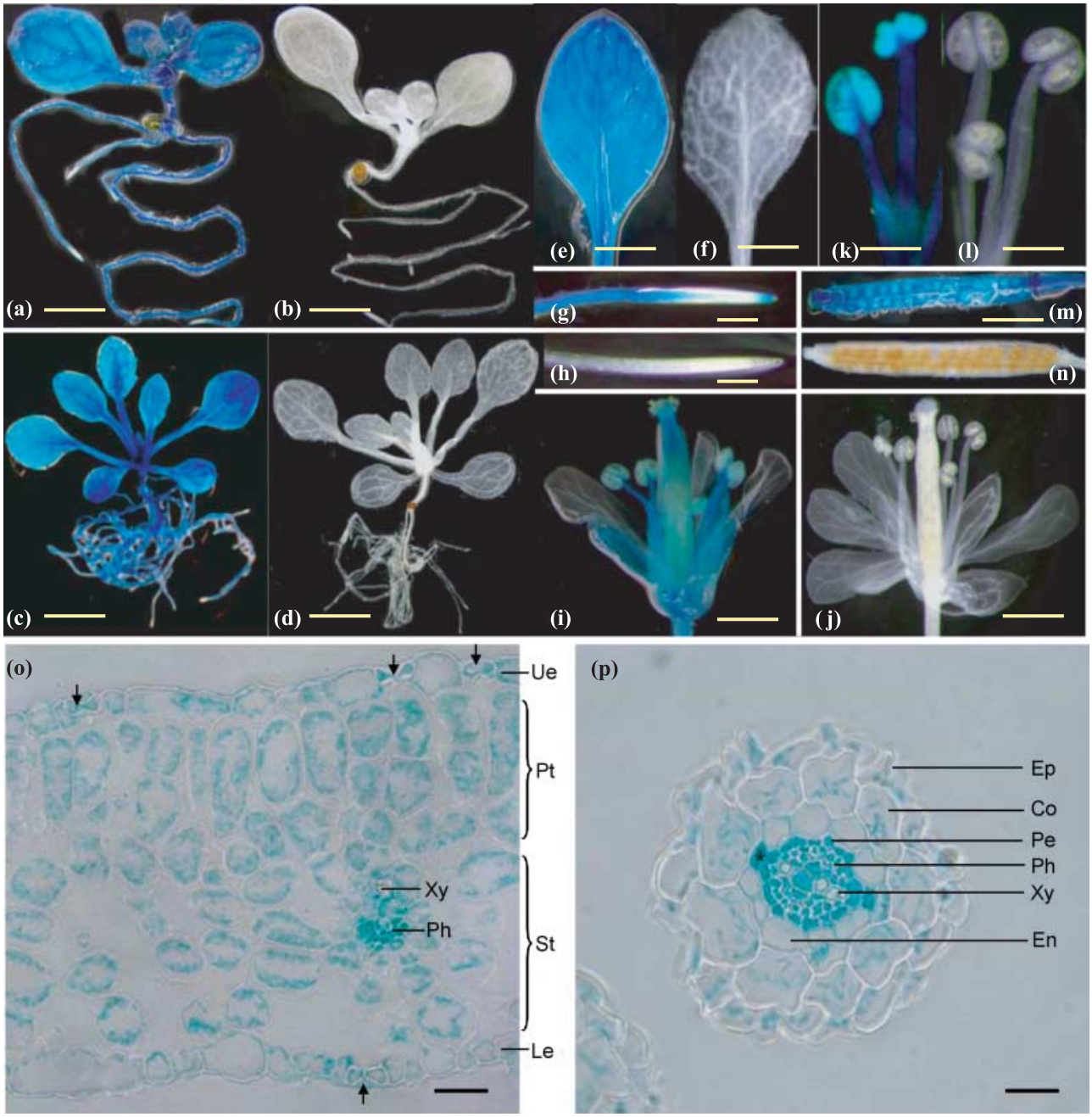

Fig. 6 Spatial and temporal expression of P_{AtIRT3}:*GUS* in transgenic *Arabidopsis thaliana* plants. The GUS staining of the T2 P_{AtIRT3}:*GUS* transgenic (a,c,e,g,i,k,m) and wild-type plants (b,d,f,h,j,l,n). (a,b) 7-d-old seedlings; (c,d) 14-d-old plants; (e,f) leaves; (g,h) root tips; (i,j) flowers; (k,l) stamens; (m,n) siliques and seeds. The cytohistological cross-section of leaf and root tissues are shown in (o) and (p), respectively. Cell types are as indicated. Arrows indicate stomata and star indicates one of the passage cells. Ep, epidermis; Co, cortex; Pe, pericycle; Ph, phloem; Xy, xylem; En, endodermis; Ue, upper epidermis; Pt, palisade tissue; St, spongy tissue; Le, Lower epidermis. Bars: (a,b,m,n), 1 mm; (c,d) , 5 mm; (e–l), 0.5 mm; (o,p), 20 μm.

nonhyperaccumulator, *A. thaliana*, Zn accumulation was enhanced. In addition, Fe accumulation enhanced in the root may indicate an as yet unknown difference in Fe–Zn homeostasis in *A. halleri*, which might be required for Fe nutrition under conditions of extreme Zn excess. The recently available transformation methodology for *A. halleri* (Hanikenne *et al.*, 2008) should provide a powerful tool for future study of *IRT3* in this regard.

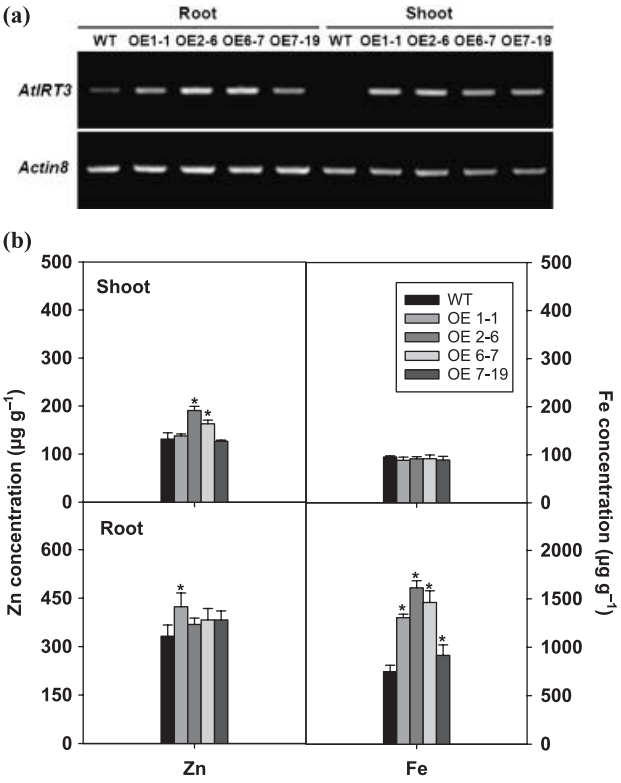

Fig. 7 Zinc (Zn) and iron (Fe) concentrations in transgenic *Arabidopsis thaliana* lines overexpressing *AtIRT3 (OE1-1, OE2-6, OE6-7, OE7-19)* and in wild-type plants (WT). (a) reverse transcriptase polymerase chain reaction (RT-PCR) of *AtIRT3* expression (24 cycles). *Actin8* served as the control (27 cycles). The Zn and Fe (b) concentrations in shoot and root tissues of 17-d-old seedlings grown in 1/2 Murashige and Skoog (MS) media. Error bars represent the standard deviation for means of three independent experiments. *, $P < 0.05$ for significant difference from controls.

Acknowledgements

This work was supported by grants from the National Science Council (93-2311-B-001-016, 93-2311-B-001-050 and 94-2311-B-001-002 to K. C. Y.) and by the Deutsche Forschungsgemeinschaft (Graduiertenkolleg 416 to S.C.). We thank Huai-Chih Chiang and Chong-Cheong Lai for technical assistance, Dr David Eide for the vector pFL61 and *S. cerevisiae* strains *zrt1zrt2* ZHY3 and *fet3fet4* DDY4, and Dr Inhwan Hwang for providing the p326GFP. We thank Dr Shu-Hsing Wu for helpful discussions.

References

Assuncao AGL, Martins PD, De Folter S, Vooijs R, Schat H, Aarts MGM. 2001. Elevated expression of metal transporter genes in three accessions of the metal hyperaccumulator *Thlaspi caerulescens*. *Plant, Cell & Environment* **24**: 217–226.

Baker AJM, Brooks RR. 1989. Terrestrial higher plants which hyperaccumulate metallic elements – a review of their distribution, ecology and phytochemistry. *Biorecovery* **1**: 81–126.

Becher M, Talke IN, Krall L, Kramer U. 2004. Cross-species microarray transcript profiling reveals high constitutive expression of metal homeostasis genes in shoots of the zinc hyperaccumulator *Arabidopsis halleri*. *Plant Journal* **37**: 251–268.

Bert V, Bonnin I, Saumitou-Laprade P, de Laguerie P, Petit D. 2002. Do *Arabidopsis halleri* from nonmetallicolous populations accumulate zinc and cadmium more effectively than those from metallicolous populations? *New Phytologist* **155**: 47–57.

Boch A, Trampczynska A, Simm C, Taudte N, Kramer U, Clemens S. 2008. Loss of Zhf and the tightly regulated zinc-uptake system SpZrt1 in *Schizosaccharomyces pombe* reveals the delicacy of cellular zinc balance. *FEMS Yeast Research* **8**: 883–896.

Bughio N, Yamaguchi H, Nishizawa NK, Nakanishi H, Mori S. 2002. Cloning an iron-regulated metal transporter from rice. *Journal of Experimental Botany* **53**: 1677–1682.

Chang S, Puryear J, Cainey J. 1993. A simple and efficient method for isolating RNA from pine trees. *Plant Molecular Biology Reporter* **11**: 113–116.

Chiang H-C, Lo J-C, Yeh K-C. 2006. Genes associated with heavy metal tolerance and accumulation in Zn/Cd hyperaccumulator *Arabidopsis halleri*: a genomic survey with cDNA microarray. *Environmental Science & Technology* **40**: 6792–6798.

Colangelo EP, Guerinot ML. 2006. Put the metal to the petal: metal uptake and transport throughout plants. *Current Opinion in Plant Biology* **9**: 322–330.

Connolly EL, Campbell NH, Grotz N, Prichard CL, Guerinot ML. 2003. Overexpression of the fro2 ferric chelate reductase confers tolerance to growth on low iron and uncovers posttranscriptional control. *Plant Physiology* **133**: 1102–1110.

Connolly EL, Fett JP, Guerinot ML. 2002. Expression of the irt1 metal transporter is controlled by metals at the levels of transcript and protein accumulation. *Plant Cell* **14**: 1347–1357.

Dahmani-Muller H, van Oort F, Balabane M. 2001. Metal extraction by *Arabidopsis halleri* grown on an unpolluted soil amended with various metal-bearing solids: A pot experiment. *Environmental Pollution* **114**: 77–84.

Eide D, Broderius M, Fett J, Guerinot ML. 1996. A novel iron-regulated metal transporter from plants identified by functional expression in yeast. *Proceedings of the National Academy of Sciences, USA* **93**: 5624–5628.

Ernst WHO, ed. 1974. *Schwermetallvegetation der erde*. Stuttgart, Germany: G. Fischer Verlag.

Forsburg SL, Sherman DA. 1997. General purpose tagging vectors for fission yeast. *Gene* **191**: 191–195.

Grotz N, Fox T, Connolly E, Park W, Guerinot ML, Eide D. 1998. Identification of a family of zinc transporter genes from *Arabidopsis* that respond to zinc deficiency. *Proceedings of the National Academy of Sciences, USA* **95**: 7220–7224.

Guerinot ML. 2000. The ZIP family of metal transporters. *Biochimica et Biophysica Acta* **1465**: 190–198.

Hanikenne M, Talke IN, Haydon MJ, Lanz C, Nolte A, Motte P, Kroymann J, Weigel D, Kramer U. 2008. Evolution of metal hyperaccumulation required cis-regulatory changes and triplication of hma4. *Nature* **453**: 391–395.

Ishimaru Y, Suzuki M, Kobayashi T, Takahashi M, Nakanishi H, Mori S, Nishizawa NK. 2005. Oszip4, a novel zinc-regulated zinc transporter in rice. *Journal of Experimental Botany* **56**: 3207–3214.

Ishimaru Y, Suzuki M, Tsukamoto T, Suzuki K, Nakazono M, Kobayashi T, Wada Y, Watanabe S, Matsuhashi S, Takahashi M *et al.* 2006. Rice plants take up iron as an Fe^{3+}-phytosiderophore and as Fe^{2+}. *Plant Journal* **45**: 335–346.

Kall L, Krogh A, Sonnhammer EL. 2007. Advantages of combined transmembrane topology and signal peptide prediction – the phobius web server. *Nucleic Acids Research* **35**: W429–432.

Kerkeb L, Mukherjee I, Chatterjee I, Lahner B, Salt DE, Connolly EL. 2008. Iron-induced turnover of the *Arabidopsis* IRT1 metal transporter requires lysine residues. *Plant Physiology* **146**: 1964–1973.

Korshunova YO, Eide D, Clark WG, Guerinot ML, Pakrasi HB. 1999. The irt1 protein from *Arabidopsis thaliana* is a metal transporter with a broad substrate range. *Plant Molecular Biology* **40**: 37–44.

Kubota H, Takenaka C. 2003. *Arabis gemmifera* is a hyperaccumulator of Cd and Zn. *International Journal of Phytoremediation* **5**: 197–201.

Lopez-Millan AF, Ellis DR, Grusak MA. 2004. Identification and characterization of several new members of the zip family of metal ion transporters in *Medicago truncatula*. *Plant Molecular Biology* **54**: 583–596.

Maser P, Thomine S, Schroeder JI, Ward JM, Hirschi K, Sze H, Talke IN, Amtmann A, Maathuis FJM, Sanders D *et al.* 2001. Phylogenetic relationships within cation transporter families of *Arabidopsis*. *Plant Physiology* **126**: 1646–1667.

Moreau S, Thomson RM, Kaiser BN, Trevaskis B, Guerinot ML, Udvardi MK, Puppo A, Day DA. 2002. Gmzip1 encodes a symbiosis-specific zinc transporter in soybean. *Journal of Biological Chemistry* **277**: 4738–4746.

Pence NS, Larsen PB, Ebbs SD, Letham DLD, Lasat MM, Garvin DF, Eide D, Kochian LV. 2000. The molecular physiology of heavy metal transport in the Zn/Cd hyperaccumulator *Thlaspi caerulescens*. *Proceedings of the National Academy of Sciences, USA* **97**: 4956–4960.

Peterson CA, Enstone DE. 1996. Functions of passage cells in the endodermis and exodermis of roots. *Physiologia Plantarum* **97**: 592–598.

Ramesh SA, Shin R, Eide DJ, Schachtman DP. 2003. Differential metal selectivity and gene expression of two zinc transporters from rice. *Plant Physiology* **133**: 126–134.

Rhodes D, Klug A. 1993. Zinc fingers. *Scientific American* **268**: 56–59, 62–55.

Rogers EE, Eide DJ, Guerinot ML. 2000. Altered selectivity in an *Arabidopsis* metal transporter. *Proceedings of the National Academy of Sciences, USA* **97**: 12356–12360.

Sheen J. 2001. Signal transduction in maize and *Arabidopsis* mesophyll protoplasts. *Plant Physiology* **127**: 1466–1475.

Talke IN, Hanikenne M, Kramer U. 2006. Zinc-dependent global transcriptional control, transcriptional deregulation, and higher gene copy number for genes in metal homeostasis of the hyperaccumulator *Arabidopsis halleri*. *Plant Physiology* **142**: 148–167.

Vallee BL, Auld DS. 1990. Zinc coordination, function, and structure of zinc enzymes and other proteins. *Biochemistry* **29**: 5647–5659.

Vert G, Briat JF, Curie C. 2001. *Arabidopsis* irt2 gene encodes a root-periphery iron transporter. *Plant Journal* **26**: 181–189.

Vert G, Grotz N, Dedaldechamp F, Gaymard F, Guerinot ML, Briat JF, Curie C. 2002. Irt1, an *Arabidopsis* transporter essential for iron uptake from the soil and for plant growth. *Plant Cell* **14**: 1223–1233.

Weber M, Harada E, Vess C, von Roepenack-Lahaye E, Clemens S. 2004. Comparative microarray analysis of *Arabidopsis thaliana* and *Arabidopsis halleri* roots identifies nicotianamine synthase, a zip transporter and other genes as potential metal hyperaccumulation factors. *Plant Journal* **37**: 269–281.

Wintz H, Fox T, Wu YY, Feng V, Chen WQ, Chang HS, Zhu T, Vulpe C. 2003. Expression profiles of *Arabidopsis thaliana* in mineral deficiencies reveal novel transporters involved in metal homeostasis. *Journal of Biological Chemistry* **278**: 47644–47653.

Zhao H, Eide D. 1996. The yeast zrt1 gene encodes the zinc transporter protein of a high-affinity uptake system induced by zinc limitation. *Proceedings of the National Academy of Sciences, USA* **93**: 2454–2458.

Supporting Information

Additional supporting information may be found in the online version of this article.

Fig. S1 Phylogenic tree of ZIP and IRT proteins.

Fig. S2 The pH effect of the complementation of *S. cerevisiae fet3fet4* mutant.

Fig. S3 Quantitative real-time polymerase chain reaction (Q-PCR) of expression of *IRT3* in roots and shoots of *A. thaliana* or rooted *A. halleri* grown in control (CK), no iron (–Fe), no zinc (–Zn) and zinc excess (+Zn) media for 5 d.

Fig. S4 The activity of AtIRT3 promoter is regulated by Zn.

Fig. S5 Dry weight of wild-type and transgenic *Arabidopsis thaliana* with overexpressed *AtIRT3*.

Fig. S6 Manganese (Mn), copper (Cu), molybdenum (Mo), magnesium (Mg) and calcium (Ca) concentrations in transgenic *Arabidopsis thaliana* lines overexpressing *AtIRT3* (*OE1-1*, *OE2-6*, *OE6-7*, *OE7-19*) and in wild-type plants (WT).

Please note: Wiley-Blackwell are not responsible for the content or functionality of any supporting information supplied by the authors. Any queries (other than missing material) should be directed to the *New Phytologist* Central Office.